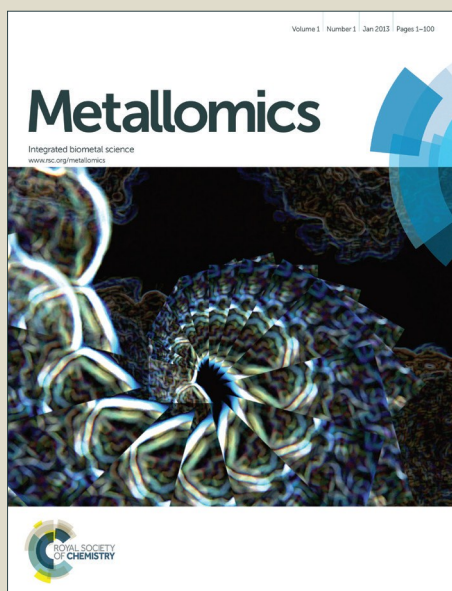


Metallomics

Accepted Manuscript



This is an *Accepted Manuscript*, which has been through the Royal Society of Chemistry peer review process and has been accepted for publication.

Accepted Manuscripts are published online shortly after acceptance, before technical editing, formatting and proof reading. Using this free service, authors can make their results available to the community, in citable form, before we publish the edited article. We will replace this *Accepted Manuscript* with the edited and formatted *Advance Article* as soon as it is available.

You can find more information about *Accepted Manuscripts* in the [Information for Authors](#).

Please note that technical editing may introduce minor changes to the text and/or graphics, which may alter content. The journal's standard [Terms & Conditions](#) and the [Ethical guidelines](#) still apply. In no event shall the Royal Society of Chemistry be held responsible for any errors or omissions in this *Accepted Manuscript* or any consequences arising from the use of any information it contains.

1
2
3
4
5
6 **Copper-responsive gene expression in the methanotroph *Methylosinus trichosporium* OB3b**
7
8
9

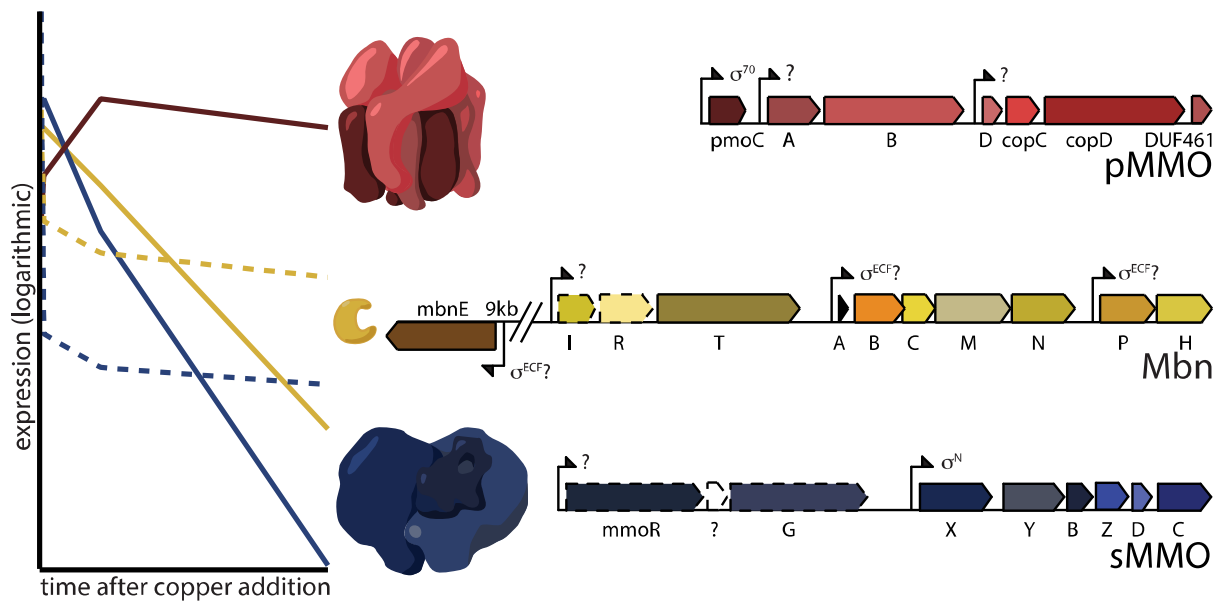
10
11
12 Grace E. Kenney^a, Monica Sadek^b, and Amy C. Rosenzweig^{a,b,1}

13 ^aDepartments of Molecular Biosciences and ^bChemistry, Northwestern University, Evanston, IL
14

15
16 60208
17
18
19
20
21
22
23
24
25
26
27

28
29 ¹To whom correspondence should be addressed. Email: amyr@northwestern.edu
30
31
32
33
34
35
36
37
38
39
40
41
42
43
44
45
46
47
48
49
50
51
52
53
54
55
56
57
58
59
60

Table of Contents Figure



Gene expression and bioinformatics studies provide new insight into copper homeostasis in the methanotroph *Methylosinus trichosporium* OB3b.

Abstract

Methanotrophic bacteria convert methane to methanol using methane monooxygenase (MMO) enzymes. In many strains, either an iron-containing soluble (sMMO) or a copper-containing particulate (pMMO) enzyme can be produced depending on copper availability; the mechanism of this copper switch has not been elucidated. A key player in methanotroph copper homeostasis is methanobactin (Mbn), a ribosomally produced, post-translationally modified natural product with a high affinity for copper. The Mbn precursor peptide is encoded within an operon that contains a range of putative transporters, regulators, and biosynthetic proteins, but the involvement of these genes in Mbn-related processes remains unclear. Extensive time-dependent qRT-PCR studies of *Methylosinus trichosporium* OB3b and the constitutive sMMO-producing mutant *Ms. trichosporium* OB3b PP358 show that the Mbn operon is indeed copper-regulated, providing experimental support for its bioinformatics-based identification. Moreover, the Mbn operon is co-regulated with the sMMO operon and reciprocally regulated with the pMMO operon. Within the Mbn and sMMO operons, a subset of regulatory genes exhibits a distinct and shared pattern of expression, consistent with their proposed functions as internal regulators. In addition, genome sequencing of the *Ms. trichosporium* OB3b PP358 mutant provides new evidence for the involvement of genes adjacent to the pMMO operon in methanotroph copper homeostasis.

Significance Statement

Methanotrophs, bacteria that convert methane gas to methanol, have attracted intense attention for their potential applications in bioremediation and gas-to-liquids conversion processes. How these bacteria obtain copper for their key metabolic enzyme, particulate methane monooxygenase (pMMO), is not well understood. One means of copper uptake involves a copper-binding natural product called methanobactin. Analysis of copper-responsive gene expression provides evidence for the involvement of specific genes in methanobactin biosynthesis, regulation, and transport as well as in the copper-dependent expression of pMMO and an alternative iron-containing, soluble MMO (sMMO). Several other genes likely involved in cytoplasmic copper uptake have also been identified.

Introduction

Methanotrophs, bacteria that are capable of subsisting on methane (CH₄) as their sole carbon and energy source¹, play a key role in the global carbon cycle, and have attracted much attention for their potential applications in bioremediation and biological gas-to-liquids conversion processes.²⁻⁴ The first step in methanotroph metabolism, the oxidation of methane to methanol, can be carried out using two entirely different enzymatic systems.¹ The more common enzyme is particulate methane monooxygenase (pMMO), a membrane protein complex that is located in intracytoplasmic and/or inner membranes⁵ and contains a copper active site.^{6,7} An alternate soluble methane monooxygenase (sMMO), located in the cytoplasm of some methanotrophs, utilizes a catalytic diiron active site.⁸ The large subset of methanotrophs that can express both MMOs exhibits a striking copper-dependent reciprocal regulation of the two operons.⁹

Previous studies broadly supported a model in which the pMMO operon, encoding the three subunits PmoA, PmoB, and PmoC, is controlled by a σ^{70} -dependent promoter (Fig. 1A), resulting in constitutive expression at an intermediate level.¹⁰⁻¹³ The operon is mildly (<10-fold) up-regulated in the presence of copper, but the regulators involved have not been identified.¹⁴⁻¹⁶ The main sMMO operon, by contrast, is controlled by a σ^N -dependent promoter, and transcription depends on the presence of two regulatory proteins, MmoR (a σ^N -dependent transcriptional activator) and MmoG (a GroEL homologue) (Fig. 1B); unlike pMMO, it is markedly down-regulated in the presence of copper, with a fold change of ten to a hundred times greater than the change observed for pMMO.^{10,13-15,17} The unknown mechanism by which these two operons are reciprocally regulated is referred to as the “copper switch,” but no evidence exists for the interaction of known copper-dependent transcriptional regulation systems with

1
2
3 either operon.¹⁸ Moreover, it is not known how copper triggers formation of the intracytoplasmic
4 membranes that house pMMO.⁴
5
6

7
8 One important agent of methanotroph copper homeostasis is methanobactin (Mbn), a small
9 peptidic copper-binding natural product (Fig. S1).¹⁹ Mbn is produced and secreted under
10 conditions of copper starvation ($< 0.8 \mu\text{M}$ soluble copper)²⁰, and is re-internalized after copper
11 binding via an active process.²¹ A putative Mbn-related operon was recently discovered,
12 including a small gene thought to encode an Mbn precursor peptide, suggesting that the
13 compound is a ribosomally produced, post-translationally modified natural product.²² This small
14 gene is repressed by copper and Mbn production is abolished when the gene is eliminated.²³
15
16 Genome mining has enabled tentative assignment of other Mbn operon components in a range of
17 species to transport, regulatory, and biosynthetic functions (Figs. 1C, S1).²⁴ However, direct
18 evidence for involvement of the additional genes in copper metabolism and Mbn-related
19 processes has not been reported.
20
21
22
23
24
25
26
27
28
29
30
31
32
33

34 Although the copper switch was first observed more than thirty years ago^{25,26}, the details of
35 copper-dependent MMO regulation and methanotroph copper metabolism, including the role of
36 Mbn, have not been elucidated²⁷. None of the three major operons appear to rely on the presence
37 of either of the others; species possessing only Mbn, pMMO, or sMMO all exist (Fig. 1D).
38
39 However, when present within the same organism, a complex copper homeostasis system
40 appears to regulate all three operons. In this study, we report extensive time-dependent qRT-PCR
41 analyses of *Methylosinus (Ms.) trichosporium* OB3b showing that the entire putative Mbn
42 operon is copper-regulated and that the sMMO and Mbn genes are co-regulated. These data
43
44 provide strong support for our identification of the Mbn operons. Moreover, genome sequencing
45
46 of a constitutive sMMO-producing mutant reveals a multi-nucleotide frameshift deletion in a
47
48
49
50
51
52
53
54
55
56
57
58
59
60

1
2
3 putative inner membrane copper importer adjacent to the pMMO operon, thus identifying
4
5 components of an additional overlapping copper homeostasis system in methanotrophs.
6
7
8
9

10 **Results and Discussion**

11
12
13
14
15 **Copper-dependent regulation of the sMMO, Mbn, and pMMO operons.** Previous
16
17 investigations of the copper switch have relied on analysis at specific static copper
18
19 concentrations. We chose to approach the copper switch as a dynamic and time-dependent
20
21 system, relying on a set of timecourse experiments to track the transition from a copper-starved
22
23 to a copper-replete state. Towards this end, samples of wildtype *Ms. trichosporium* OB3b were
24
25 taken prior to the addition of copper to a final concentration of 12.5 μ M and at 15 min, 5 h, and
26
27 24 h after copper addition. Normalized relative expression levels show several clear trends.
28
29 Transcript levels of the main sMMO operon (*mmoRGXYBZDC*) drop significantly by 5 h, and
30
31 are down-regulated by 2-3 orders of magnitude over the 24 h time period (Figs. 2, S2). This
32
33 downregulation has been observed previously via proteomics¹⁵ as well as detection of the *mmoX*
34
35 mRNA^{10,14}. Most important, copper-responsive regulation of the Mbn operon parallels that of
36
37 sMMO. Transcript levels for the entire putative Mbn operon, *mbnIRTABCMNPH*, as well as
38
39 *mbnE*, located approximately 9kb upstream of *mbnIRT* (Fig. 1C), also drop significantly by 5 h
40
41 and are down-regulated by 1-2 orders of magnitude over 24 hrs (Figs. 2, S2). The
42
43 downregulation of *mbnA* as well as all the other genes by copper is consistent with MbnA being
44
45 the Mbn precursor peptide and with the entire operon functioning in copper acquisition: as
46
47 copper concentrations increase, Mbn production decreases,²⁸ and accordingly its regulatory,
48
49 transport, and biosynthetic machinery is no longer highly expressed. Given that some or all of
50
51
52
53
54
55
56
57
58
59
60

1
2
3 these genes are conserved in a range of Mbn operons,²⁴ it is likely that these proteins have Mbn-
4 related functions in other organisms as well.
5
6

7
8 In contrast to the sMMO operon, copper-responsive regulation of pMMO has been somewhat
9 controversial. Unlike sMMO, there is a considerable basal level of constitutive expression,
10 mediated by a σ^{70} promoter.¹¹⁻¹³ Some studies show little change in response to copper,^{10,29} some
11 show a mild increase,^{9,15,16} and several suggest a significant increase.^{23,30} Our data show that
12 genes in the pMMO operon are mildly up-regulated by less than an order of magnitude over 24 h
13 (Figs. 2, S2). These results are consistent with a consensus model in which mild up-regulation of
14 the pMMO operon does occur in the presence of copper, with the possibility of a post-
15 transcriptional regulatory step still open.
16
17

18
19 In other studies, a range of phenotypes have been used as proxies for identifying whether a
20 given methanotroph cell population is in low- or high-copper mode, including the presence of
21 intracytoplasmic membranes (ICMs).^{5,31} the naphthalene activity assay (limited to sMMO-
22 producing strains),³² and secretion of Mbn into the spent medium (in species that produce
23 Mbn).²⁸ In our timecourse experiments, these phenotypes clearly track with the mRNA levels
24 observed in the qRT-PCR analysis (Fig. 3). Metal free (apo) Mbn is visible in the spent medium
25 at the 0 min timepoint, but has shifted to copper-loaded Mbn 15 min after copper addition (Figs.
26 3, S3). Intracellular membranes are detected primarily at the 5 h and 24 h timepoints, and
27 naphthalene oxidation by sMMO clearly decreases at the later timepoints (Fig. 3).
28
29

30
31 **The sMMO and Mbn regulatory genes.** Further examination of the qRT-PCR data indicates
32 that genes within the sMMO and Mbn operons exhibit two distinct regulatory patterns. Both
33 operons are clearly down-regulated by copper, but the genes encoding regulatory proteins within
34
35
36
37
38
39
40
41
42
43
44
45
46
47
48
49
50
51
52
53
54
55
56
57
58
59
60

1
2
3 the sMMO operon, *mmoR*, an uncharacterized and previously unnoted but well-conserved ORF
4 with the current locus tag MettrDRAFT_0733, and *mmoG*,¹⁶ along with the proposed regulatory
5 protein genes *mbnI* and *mbnR* in the Mbn operon²⁴ are down-regulated within 15 min (Figs. 2,
6 S2). By contrast, the rest of the operon components show no significant response over this time
7 range, with expression levels dropping only by the 5 h and 24 h timepoints. This observation is
8 consistent with a model in which the main operons are controlled by their internal regulators,
9 which are the primary targets of copper or other copper-dependent regulatory proteins.

10
11
12
13
14
15
16
17
18
19
20 MbnI is an extracytoplasmic function (ECF) sigma factor that has already been proposed as a
21 potential regulator for the Mbn operon, and possibly for the copper switch as well.²⁴ Analogous
22 ECF sigma factors in siderophore systems are partnered with inner-membrane anti-sigma factors
23 that interact with TonB-dependent transporters to form a cell surface to cytoplasm signal
24 transduction cascade.³³⁻³⁶ The MbnIRT triad comprises a potentially similar system, which
25 would couple Mbn import to Mbn regulation. In this model, MbnI would not bind copper or
26 Mbn, but would rather interact directly with the inner membrane anti-sigma factor MbnR and its
27 target regulatory region in response to Mbn uptake by MbnT.²⁴ To further assess the regulatory
28 role of MbnI, MbnI was cloned, heterologously expressed, and purified. MbnI with a C-terminal
29 Strep-Tactin tag expresses as a monomer and binds no metal ions as measured by ICP-MS,
30 which is consistent with its role as part of a sigma/anti-sigma factor system. However, it does
31 bind to a heparin column, a frequently used proxy for DNA binding (Fig. S4).³⁷ This initial
32 characterization is consistent with its predicted role as an ECF sigma factor. Bioinformatic
33 analyses and gel-shift trials involving the regions preceding MbnA, MbnI, and potentially other
34 Mbn-related genes across methanotroph species have been inconclusive; identification of the
35 MbnI recognition site and regulon will require further investigation.

1
2
3
4
5
6
7
8
9
10
11
12
13
14
15
16
17
18
19
20
21
22
23
24
25
26
27
28
29
30
31
32
33
34
35
36
37
38
39
40
41
42
43
44
45
46
47
48
49
50
51
52
53
54
55
56
57
58
59
60

Besides MmoR and MmoG, an additional component of the sMMO operon, MmoD, has been proposed as a regulator for the copper switch.²³ Early studies indicated that MmoD interacts directly with the sMMO hydroxylase, inhibiting activity *in vitro*,³⁸ but based on recent studies of an *Ms. trichosporium* OB3b $\Delta mmoXYBZDC_{1-3}$ mutant, it was proposed to be a copper-dependent regulatory protein²³ However, *mmoD* is not down-regulated with the other sMMO and Mbn regulatory genes, and methanotroph MmoD proteins lack well-conserved and characterized DNA-binding and metal-binding motifs. To further probe this proposed regulatory role, we heterologously expressed and purified MmoD with a C-terminal Strep-Tactin tag. We observe more of the monomeric form than reported previously,³⁸ possibly due to a swifter purification process and a different set of affinity tags. Whether produced without metal supplementation or isolated from cells grown with 5 mM CuSO₄, no significant copper binding is observed via ICP-MS, and under no conditions does MmoD appear to bind a heparin column (Fig. S4). These combined data support the preliminary identification of MbnI, but not MmoD, as a DNA binding protein with potential relevance to copper homeostasis. However, understanding the roles of both proteins will require extensive further investigation.

The constitutive sMMO-expressing mutant *Ms. trichosporium* OB3b PP358. In 1992, a series of constitutively sMMO-expressing strains of *Ms. trichosporium* OB3b were generated via treatment with dichloromethane, a suicide inhibitor of pMMO as well as a mutagen.³⁹ The five final strains (PP311, PP319, PP323, PP333 and PP358) have certain shared phenotypes: they express sMMO even at copper concentrations > 5 μ M, and exhibit decreased levels of total cellular copper.⁴⁰ A comparison of copper levels in the particulate and soluble fractions of lysed cells suggests that much of that decrease derives from the lack of pMMO, which as a

1
2
3 cuproenzyme comprising a large portion of the cellular protein mass represents a significant
4 fraction of the copper pool.^{25,26,40} However, copper levels in the soluble fractions, including
5
6 cytoplasmic and periplasmic proteins, are also decreased.
7
8
9

10 These constitutive sMMO-producing mutants were thus suggested to be defective in either
11 copper acquisition or copper regulation of the two MMOs.²⁸ Notably, secretion of a copper-
12 binding compound, later characterized and identified as Mbn, was first observed in these strains,
13 although it was later also identified in the wildtype species.⁴⁰ We extended our gene expression
14 studies to the mutant strain *Ms. trichosporium* OB3b PP358 with the goal of detecting
15 differential gene regulation that could be linked to altered pathways. Although the continued
16 presence of high levels of the *mmoXYBZDC* portion of the sMMO operon is expected from the
17 phenotype, Mbn was uncharacterized at the time of PP358 development, and few experiments
18 were carried out above 5 μ M copper, meaning that a copper response differing from the response
19 patterns of sMMO could not be ruled out.
20
21
22
23
24
25
26
27
28
29
30
31
32
33

34 The striking down-regulation of the full sMMO and Mbn operons was not observed in PP358
35 (Figs. 2, S2), although a significantly dampened copper response is eventually visible in some
36 samples; this provides further support for the co-regulation of the sMMO and Mbn operons. As
37 expected, sMMO activity and Mbn production are detected at high copper concentrations, and
38 Mbn from PP358 had the same mass as the compound produced by the wildtype organism (Figs.
39 3, S3). Similarly dampened responses were observed for the pMMO operon, and the formation
40 of significant numbers of intracytoplasmic membranes was not observed (Figs. 2, 3). These
41 trends verified and further characterized the PP358 phenotype while eliminating some possible
42 causes, but its origin remained unclear.
43
44
45
46
47
48
49
50
51
52
53
54
55
56
57
58
59
60

1
2
3 We then used next-generation sequencing to compare the PP358 genome to the published
4
5 *Ms. trichosporium* OB3b genome.⁴¹ High levels of coverage (130-170x) were obtained across the
6
7 entire genome, which enabled detailed identification of variants including insertions, deletions,
8
9 and single nucleotide polymorphisms (Supplemental File S1). Of high-likelihood variants that
10
11 did not represent silent mutations, a significant number were in genes and genomic regions
12
13 unlikely to be related to methane or copper metabolism (particularly genes related to mobile
14
15 genetic elements, including transposases and related machinery). A smaller subset retained some
16
17 plausible relevance to copper homeostasis (Table S1). One variant in particular stood out: a
18
19 multi-nucleotide frameshift deletion in a gene encoding CopD, an inner membrane protein
20
21 thought to be responsible for importing copper into the cytoplasm in many bacterial species.⁴²⁻⁴⁵
22
23 Sanger sequencing of a PCR-amplified fragment containing this region confirmed the presence
24
25 of this deletion (Fig. 4A). TopCons⁴⁶ predicts that wildtype CopD contains 10 transmembrane
26
27 helices and a C-terminal periplasmic domain. The deletion causes a frame shift in the gene,
28
29 resulting in the eradication of the final transmembrane helix and the C-terminal periplasmic
30
31 domains (Fig. 4B).
32
33
34
35
36
37
38

39 Strikingly, the *copD* gene in *Ms. trichosporium* OB3b is located two genes downstream of
40
41 one copy of the pMMO *pmoCAB* operon, preceded by the *pmoD* and *copC* genes and followed
42
43 by a gene denoted *DUF461* (Fig. 1A). The presence of additional genes has been noted
44
45 previously in some operons encoding ammonia monooxygenase (AMO), a pMMO homolog, in
46
47 which genes of unknown function follow *amoCAB*: *amoD*, which is a *pmoD* homolog, and in
48
49 some cases *amoE*, a more distant *pmoD* homolog.^{47,48} In beta-proteobacterial ammonia oxidizers
50
51 and alpha-proteobacterial methanotrophs, including *Ms. trichosporium* OB3b, the *amoD/pmoD*
52
53 genes are followed by *copC*, which encodes a periplasmic copper binding protein CopC⁴⁹⁻⁵¹,
54
55
56
57
58
59
60

1
2
3 *copD*^{42,43,50}, and *DUF461*, which encodes a second putative periplasmic copper chaperone
4 related to PCu_AC, ECuC, and other proteins thought to be involved in cytochrome *c* oxidase
5 copper loading.⁵²⁻⁵⁴ Like pMMO, all four of these genes are mildly up-regulated in the presence
6 of copper (Figs. 2, S2); interestingly, a *pmoD* homologue (MCA2130) was also recently
7 identified as part of the copper-upregulated transcriptome in microarray studies of
8 *Methylococcus capsulatus* (Bath).¹⁴
9
10
11
12
13
14
15
16

17 The *copD* genes from the few studied proteobacterial *copCD* operons^{42,43,50,55} are predicted
18 by TopCons and TMHMM to encode proteins that include eight transmembrane helices. Several
19 potential copper-binding residues, including histidines, are conserved in predicted periplasmic
20 loop regions (Fig. S5, Supplemental Results and Discussion). By contrast, *copD* genes found
21 following alpha-proteobacterial pMMO and beta-proteobacterial AMO operons contain an extra
22 two transmembrane helices and a C-terminal periplasmic domain with a predicted heme binding
23 site annotated as a cytochrome *cbb3*-like domain (PF13442, corresponding to the CcoP/FixP
24 subunit of the enzyme (Fig. S5)). Of the 10,887 genes containing *copD* domains found in the JGI
25 database at the time of analysis, only 42 genes include the cytochrome *cbb3*-like domain, and of
26 those, 27 are from alpha-proteobacterial ammonia oxidizers or beta-proteobacterial
27 methanotrophs. Gamma-proteobacterial methanotrophs and ammonia oxidizers do not have a
28 *copD* gene in the immediate proximity of their AMO/pMMO operons, but they almost invariably
29 possess *copCD* pairs elsewhere in their genomes. These gamma-proteobacterial *copD*
30 homologues are predicted to have 14 transmembrane helices, and the extra 6 helices are part of a
31 C-terminal domain with some homology to the cytochrome *c* oxidase *caa3* assembly factor
32 (CtaG), which is thought to be involved in the correct assembly of the Cu_A site of *Bacillus*
33 *subtilis* cytochrome *c* oxidase *caa3* (not to be confused with the Cox11 homologue known as
34
35
36
37
38
39
40
41
42
43
44
45
46
47
48
49
50
51
52
53
54
55
56
57
58
59
60

1
2
3 CtaG that is found in *Rhodobacter sphaeroides* and *Paracoccus denitrificans*).^{56,57} As with the
4
5 C-terminal *cbb3*-like domain, this domain is particularly well represented in methanotrophs and
6
7 ammonia oxidizers, and interestingly, a variant with 16 helices is also common in gram positive
8
9 bacteria (Fig. S5). Many species possess multiple *copCD* pairs in their genomes, potentially
10
11 consistent with these proteins playing a range of roles.
12
13
14

15 The involvement of CopD in the copper switch would have several important implications
16
17 for methanotroph copper regulation. First, impaired copper import into the cytoplasm will affect
18
19 cytoplasmic metal-binding regulatory proteins, but not regulatory mechanisms that involve
20
21 periplasmic metal sensors, ruling out two-component regulatory systems⁵⁸ as likely copper
22
23 switch regulators. Second, increased periplasmic copper due to reduced cytoplasmic uptake
24
25 might result in up-regulation of export systems; for characterized copper resistance systems in
26
27 gram-negative bacteria, regulation frequently depends on periplasmic copper sensing via two-
28
29 component regulators such as CusRS, PcoRS, and CopRS.^{59,60} There are no *copABCDRS*
30
31 operons in *Ms. trichosporium* OB3b,⁴¹ but *cus*-like RND export systems of unknown metal
32
33 specificity are present,⁴¹ and PP358 has been previously observed to have a low copper content
34
35 compared to wildtype *Ms. trichosporium* OB3b at the same external copper level.⁴⁰ Finally,
36
37 cytoplasmic copper import may not only impact copper regulation, but may also play a role in
38
39 assembly of the pMMO active site analogous to what has been proposed for cytochrome *c*
40
41 oxidase.⁶¹⁻⁶³
42
43
44
45
46
47
48
49
50

51 Conclusions

52
53 These data fill in a number of gaps in our current understanding of methanotroph copper
54
55 homeostasis (Fig. 5). First, the full putative Mbn operon is coregulated with the precursor
56
57
58
59
60

1
2
3 peptide, MbnA, and both are significantly down-regulated in the presence of copper, providing
4 strong support for the bioinformatics-based identification of the Mbn operons as well as the
5 assignment of the broader class of Mbn operons, present not only in methanotrophs but in a
6 range of other bacterial species.²⁴ Second, the Mbn and sMMO operons are co-regulated,
7 suggesting that they are indeed ultimately controlled by the same copper-responsive transcription
8 factor. In *Ms. trichosporium* OB3b, the regulatory genes in each operon are swiftly down-
9 regulated after the addition of copper, and the main operons follow more slowly, consistent with
10 a regulatory mode in which the in-operon regulators activate sMMO expression and Mbn
11 biosynthesis, and are themselves repressed immediately upon copper addition, resulting in a
12 slower decline in sMMO and Mbn as available regulator protein levels fall. Third, the mutation
13 of the *copD* gene in the constitutive sMMO-producing strain PP358 provides new evidence for
14 the involvement in a second set of copper-related genes located downstream of the pMMO
15 operon in methanotroph copper homeostasis. The specific regulator(s) responsible for the copper
16 switch has not yet been identified, but these combined findings provide a strong framework and
17 many new directions for future study.
18
19
20
21
22
23
24
25
26
27
28
29
30
31
32
33
34
35
36
37
38
39
40

41 **Materials and Methods**

42
43
44 Additional experimental procedures are provided in SI Materials and Methods.
45
46
47
48

49 **Bacterial strains and medium.** Copper-starved wildtype *Ms. trichosporium* OB3b as well as the
50 mutant strain PP358 (ATCC 55314)³⁹ were grown in 50 mL cultures as described previously.²¹
51
52 Larger cultures were grown in spinner flasks specially adapted for methanotroph growth.
53
54
55
56 Glassware, including spinner flasks, was treated overnight with 5% trace metal-grade nitric acid,
57
58
59
60

1
2
3 rinsed thoroughly and autoclaved once with MilliQ-grade H₂O, and a second time dry. Standard
4
5 and low-copper growth media and gas mixtures were prepared as described previously.²¹
6
7
8
9

10 **Timecourse experimental design.** All experiments were performed with three independent
11 biological replicates. Cultures were monitored for transition into mid-logarithmic phase growth
12 (0.6 < O.D. < 1.0) and assayed for Mbn production and sMMO activity to confirm the correct
13 starting phenotype. Once cultures achieved logarithmic growth, cells were harvested from
14 spinner flasks prior to addition of CuSO₄ to a final concentration of 12.5 μM, as well as 15 min,
15 5 h, and 24 h after copper addition. At each timepoint, cells were harvested for RNA isolation
16 (see SI), OD measurement, UV-visible spectroscopy of spent medium, and transmission electron
17 microscopy (TEM).
18
19
20
21
22
23
24
25
26
27
28
29
30

31 **qRT-PCR.** All qRT-PCR primers (IDT) were designed using the IDT PrimerQuest tool and
32 were selected using constraints including $60^{\circ}\text{C} \leq T_m \leq 64^{\circ}\text{C}$, $\Delta G_{\text{homodimer}} \geq -7.5$, $\Delta G_{\text{heterodimer}} \geq -$
33 7.5 , and $\Delta G_{\text{hairpin}} \geq -3$, amplicon length between 70 and 150bp, and no products with fewer than 5
34 mismatches and 1-2 gaps identified in the target genome using e-PCR (NCBI) (Table S3). Each
35 set of qRT-PCR reactions was prepared in white Bio-Rad 384-well PCR plates, and each
36 reaction contained 1.2 μL SYBR GreenER Express Universal Master Mix (Invitrogen) and 1.2
37 μL of varying amounts of cDNA (1 ng for standard reactions and fourfold dilutions from 2ng to
38 488fg for primer efficiency runs), high-quality RNA (Table S4), and/or water, dispensed via a
39 Mosquito HTS liquid handling device (TTP), as well as 90 nL pooled forward and reverse
40 primers (5 μM each), dispensed via an Echo liquid handler (LabCyte). Each reaction was
41 prepared with on-plate technical triplicates, as well as no-template controls (NTC) and no-
42
43
44
45
46
47
48
49
50
51
52
53
54
55
56
57
58
59
60

1
2
3 reverse-transcriptase (NRT) controls, also performed in triplicate for each primer set (NTC) or
4 sample/primer combination (NRT). Reactions were incubated at 4 °C for 1 h, and then were run
5
6 on a CFX384 (Bio-Rad), with an initial 2 m UDG inactivation step at 50 °C, followed by 2 m at
7
8 95 °C. This was followed by 40 cycles of 95 °C for 15 s and 60 °C for 1 m, with plate reading
9
10 occurring during the combined annealing/extension step. After qRT-PCR was complete,
11
12 samples were allowed to anneal at 50 °C for 1 m, and melt curves were obtained by performing a
13
14 plate reading step for 5 s every 0.5 ° from 50 °C to 95 °C. Cq values were determined in the Bio-
15
16 RAD CFX software using regression for each trace. Outliers that had no Cq (in replicates where
17
18 other samples had a Cq) or a melting curve not corresponding to the peak of the product were
19
20 removed in the Bio-Rad software; other outliers were addressed during analysis with
21
22 qBASE^{PLUS}. In rare cases where significant gDNA contamination was observed (Cq values and
23
24 products with the correct melting curve for multiple replicates and multiple genes in a given
25
26 sample), the remaining RNA was treated again with Turbo DNAFree (Ambion), re-quantified,
27
28 reverse transcribed again, and re-analyzed.
29
30
31
32
33
34
35

36 To confirm the existence of a single, correctly-sized product, larger 5 µL qRT-PCR reactions
37
38 were performed under the same conditions and run on a 4% NuSieve 3:1 agarose gel in TBE
39
40 (Lonza) (Fig. S6). Similarly, since all qRT-PCR reactions were conducted using SYBR Green to
41
42 visualize product accumulation, melting curves were determined for all reactions. Primers (and,
43
44 ultimately, reference gene candidates) that exhibited multiple melting peaks or multiple bands on
45
46 the analytical agarose gel (Fig. S6) were removed from candidacy. The sequences, product sizes,
47
48 and locus tags for genes of interest and reference gene candidates are provided in Table S2.
49
50
51
52
53
54
55
56
57
58
59
60

1
2
3
4 **Quantification of relative gene expression levels.** Initial data screening, including visualization
5 of melt curves, was performed in the CFX Manager software 3.1 (Bio-Rad); at this stage,
6 reactions with no signal or a signal over 10 Cq from those of its technical replicates were
7 removed from further calculations if the remaining technical replicates were acceptable. Primer
8 efficiency calculation (Table S5), identification of acceptable reference genes (Fig. S7), and
9 calculation of CNRQ for all genes was performed in GeNorm^{PLUS}/qBase^{PLUS} 3.0 (Biogazelle)^{64,65}
10 (Supplemental File S2). Hierarchical clustering of log₁₀-transformed CNRQ data was performed
11 as described in Cluster 3.0⁶⁶, and dendrograms and heatmaps were generated from this data using
12 JavaTreeView.⁶⁷
13
14
15
16
17
18
19
20
21
22
23
24
25
26

27 **Phenotype analysis.** At each time point, 1 mL methanotroph culture was subjected to
28 centrifugation for 15 min at 8000 x g at room temperature, and a UV-visible light spectrum was
29 obtained from the supernatant using an Agilent 8453 UV-visible spectrophotometer. The sMMO
30 activity assay was performed as previously described, except that cells were washed three times
31 in salt solution prior to naphthalene incubation, and a saturating amount of naphthalene was
32 added directly to cell suspensions.^{32,68} For TEM, approximately 3E9 cells (calculated via culture
33 optical density) were collected via centrifugation for 20 min at 6000 x g and 4 °C. The pellet was
34 resuspended in growth medium without metals but containing 5% EM grade glutaraldehyde
35 (Sigma) and incubated for 4 h at 4°C while rocking. At that time, the cells were re-pelleted and
36 re-suspended in fresh phosphate/glutaraldehyde buffer and incubated overnight at 4 °C while
37 rocking. The cells were centrifuged again and the resulting pellet was further fixed with 2
38 exchanges of a modified Karnovsky's formula (2.5% glutaraldehyde, 2% paraformeldehyde in a
39 0.05M PBS). The fixed bacteria were rinsed 3x in 0.05 M PBS. Enrobed bacteria
40
41
42
43
44
45
46
47
48
49
50
51
52
53
54
55
56
57
58
59
60

1
2
3 were embedded in resin, sectioned, and imaged using Gatan Orius camera on a JEOL 1230 TEM
4
5 (80kV accelerating voltage) (Additional methods in SI).
6
7
8
9

10 **Genomic DNA isolation, library preparation, and sequencing.** Cells of copper-starved *Ms.*
11 *trichosporium* OB3b PP358 were harvested, and the MasterPure Complete DNA Isolation kit
12 (Epicentre) was used as described to isolate genomic DNA. dsDNA was quantified on a QuBit.
13
14 When excess RNA was detected, a second RNase A (Epicentre) incubation was performed,
15 followed by a phenol-chloroform extraction to remove the enzyme and a final clean-up step
16 using a Genomic DNA Clean & Concentrator kit (Zymo Research). dsDNA was quantified using
17 a QuBit prior to library construction.
18
19
20
21
22
23
24
25
26

27 Three separate gDNA libraries were prepared and sequenced. A 500 bp short insert library
28 and a 2 kb mate pair library were prepared using TruSeq and Nextera Mate Pair kits respectively
29 (Illumina) and were sequenced on an Illumina HiSeq2000 using 100bp paired-end reads (Beijing
30 Genomics Institute). The reads were filtered to remove reads with more than 10% uncalled bases
31 and reads in which at least 40% of the bases had phred scores under 20. Reads with adapter
32 contamination were also removed.
33
34
35
36
37
38
39
40

41 Reads from all three datasets were aligned to *Ms. trichosporium* OB3b using BWA MEM
42 with default parameters. The resulting BAM file was sorted and variants were discovered using
43 the Samtools mpileup function (version 1.2) followed by BCFtools (version 1.2) using standard
44 parameters. Variants having a Quality score less than 20 or a read depth greater than 350 were
45 flagged as low quality, and identified variants were manually confirmed using IGV 2.3.55.⁶⁹ To
46 confirm regions of particular interest, Sanger sequencing was employed on PCR-generated
47
48
49
50
51
52
53
54
55
56
57
58
59
60

1
2
3 fragments (sequences in Table S6). The resulting nucleotide sequences were aligned against the
4
5 wildtype DNA sequence using MAFFT (L-INS-I mode).⁷⁰
6
7
8
9

10 **CopD bioinformatics.** All ORFs containing the CopD PFAM (PF05425) were obtained from the
11
12 JGI-IMG database (Supplemental Files S3, S4). The predicted number of helices was calculated
13
14 using TMHMM.⁷¹ For genes of interest, including CopD from wildtype and mutant *Ms.*
15
16 *trichosporium* OB3b PP358, transmembrane homology was confirmed via TopCons,⁴⁶ and the
17
18 JGI-IMG annotation of additional domains was supplemented by analysis with HHPred⁷² (SI
19
20 textfile 2).
21
22
23
24
25
26

27 **Acknowledgements**

28
29 This work was supported by NSF grant MCB0842366 and the Institute for Sustainability and
30
31 Energy at Northwestern (ISEN). G.E.K. was supported by American Heart Association
32
33 predoctoral fellowship 14PRE20460104 and the Northwestern University Presidential
34
35 Fellowship. Imaging work was performed at the Biological Imaging Facility generously
36
37 supported by the Office for Research (Northwestern University). The qRT-PCR experiments
38
39 were performed at the High Throughput Analysis Facility, supported by the Robert H. Lurie
40
41 Cancer Center and the Office for Research (Northwestern University). Nucleic acid quality
42
43 control and genome sequencing were performed with the help of the NUSeq Core Facility
44
45 (Northwestern University.) Mass spectrometry was performed at the Integrated Molecular
46
47 Structure Education and Research Center. We additionally thank Dr. George Georgiou for
48
49 permission to use the PP358 strain (sourced from ATCC) and Dr. Stefan Green (University of
50
51 Illinois, Chicago) for assistance with the PP358 genome.
52
53
54
55
56
57
58
59
60

References

- 1 S. Sirajuddin and A. C. Rosenzweig, *Biochemistry*, 2015, **54**, 2283–2294.
- 2 J. D. Semrau, *Front Microbiol*, 2011, **2**, 209.
- 3 C. A. Haynes and R. Gonzalez, *Nature Chem Biol*, 2014, **10**, 331–339.
- 4 R. S. Hanson and T. E. Hanson, *Microbiol Rev*, 1996, **60**, 439–471.
- 5 C. A. Brantner, C. C. Remsen, H. A. Owen, L. A. Buchholz and M. L. Perille Collins, *Arch Microbiol*, 2002, **178**, 59–64.
- 6 R. L. Lieberman and A. C. Rosenzweig, *Nature*, 2005, **434**, 177–182.
- 7 R. Balasubramanian, S. M. Smith, S. Rawat, L. A. Yatsunyk, T. L. Stemmler and A. C. Rosenzweig, *Nature*, 2010, **465**, 115–119.
- 8 A. C. Rosenzweig, C. A. Frederick, S. J. Lippard and P. Nordlund, *Nature*, 1993, **366**, 537–543.
- 9 A. K. Nielsen, K. Gerdes and J. C. Murrell, *Mol Microbiol*, 1997, **25**, 399–409.
- 10 M. H. Ali and J. C. Murrell, *Microbiology*, 2009, **155**, 761–771.
- 11 B. Gilbert, I. R. McDonald, R. Finch, G. P. Stafford, A. K. Nielsen and J. C. Murrell, *Appl Environ Microbiol*, 2000, **66**, 966–975.
- 12 S. Stolyar, M. Franke and M. E. Lidstrom, *J Bacteriol*, 2001, **183**, 1810–1812.
- 13 G. P. Stafford, J. Scanlan, I. R. McDonald and J. C. Murrell, *Microbiology*, 2003, **149**, 1771–1784.
- 14 Ø. Larsen and O. A. Karlsen, *MicrobiologyOpen*, 2015, 1–14.
- 15 W.-C. Kao, Y.-R. Chen, E. C. Yi, H. Lee, Q. Tian, K.-M. Wu, S.-F. Tsai, S. S.-F. Yu, Y.-J. Chen, R. Aebersold and S. I. Chan, *J Biol Chem*, 2004, **279**, 51554–51560.

- 1
2
3
4
5
6
7
8
9
10
11
12
13
14
15
16
17
18
19
20
21
22
23
24
25
26
27
28
29
30
31
32
33
34
35
36
37
38
39
40
41
42
43
44
45
46
47
48
49
50
51
52
53
54
55
56
57
58
59
60
- 16 D. W. Choi, R. C. Kunz, E. S. Boyd, J. D. Semrau, W. E. Antholine, J.-I. Han, J. A. Zahn, J. M. Boyd, A. M. de La Mora and A. A. DiSpirito, *J Bacteriol*, 2003, **185**, 5755–5764.
- 17 H. Iguchi, H. Yurimoto and Y. Sakai, *FEMS Microbiol Lett*, 2010, **312**, 71–76.
- 18 S. H. Stanley, S. D. Prior, D. J. Leak and H. Dalton, *Biotechnol Lett*, 1983, **5**, 487–492.
- 19 H. J. Kim, D. W. Graham, A. A. DiSpirito, M. A. Alterman, N. Galeva, C. K. Larive, D. Asunskis and P. M. A. Sherwood, *Science*, 2004, **305**, 1612–1615.
- 20 N. L. Bandow, W. H. Gallagher, L. A. Behling, D. W. Choi, J. D. Semrau, S. C. Hartsel, V. S. Gilles and A. A. DiSpirito, in *Methods in Methane Metabolism, Part B, 1, (2011) 1-14*. doi:10.1016/B978-0-12-386905-0.00001-2, *Methods in enzymology*, 2011, vol. 495, pp. 259–269.
- 21 R. Balasubramanian, G. E. Kenney and A. C. Rosenzweig, *J Biol Chem*, 2011, **286**, 37313–37319.
- 22 B. D. Krentz, H. J. Mulheron, J. D. Semrau, A. A. DiSpirito, N. L. Bandow, D. H. Haft, S. Vuilleumier, J. C. Murrell, M. T. McEllistrem, S. C. Hartsel and W. H. Gallagher, *Biochemistry*, 2010, **49**, 10117–10130.
- 23 J. D. Semrau, S. Jagadevan, A. A. DiSpirito, A. Khalifa, J. Scanlan, B. H. Bergman, B. C. Freemeier, B. S. Baral, N. L. Bandow, A. Vorobev, D. H. Haft, S. Vuilleumier and J. C. Murrell, *Environ Microbiol*, 2013, **15**, 3077–3086.
- 24 G. E. Kenney and A. C. Rosenzweig, *BMC Biol*, 2013, **11**, 17.
- 25 K. Takeda and K. Tanaka, *Anton Leeuw Int J G*, 1980, **46**, 15–25.
- 26 S. D. Prior and H. Dalton, *Microbiology*, 1985, **131**, 155–163.
- 27 J. D. Semrau, A. A. DiSpirito and S. Yoon, *FEMS Microbiol Rev*, 2010, **34**, 496–531.
- 28 A. A. DiSpirito, J. A. Zahn, D. W. Graham, H. J. Kim, C. K. Larive, T. S. Derrick, C. D.

- 1
2
3 Cox and A. Taylor, *J Bacteriol*, 1998, **180**, 3606–3613.
4
5
6 29 A. Vorobev, S. Jagadevan, B. S. Baral, A. A. DiSpirito, B. C. Freemeier, B. H. Bergman, N.
7
8 L. Bandow and J. D. Semrau, *Appl Environ Microbiol*, 2013, **79**, 5918–5926.
9
10 30 C. W. Knapp, D. A. Fowle, E. Kulczycki, J. A. Roberts and D. W. Graham, *Proc Nat Acad*
11
12 *Sci USA*, 2007, **104**, 12040–12045.
13
14
15 31 D. C. Scott, J. Brannan and I. J. Higgins, *J Gen Microbiol*, 1981, **125**, 63–72.
16
17 32 G. A. Brusseau, H. C. Tsien, R. S. Hanson and L. P. Wackett, *Biodegradation*, 1990, **1**, 19–
18
19 29.
20
21
22 33 B. Van Hove, H. Staudenmaier and V. Braun, *J Bacteriol*, 1990, **172**, 6749–6758.
23
24 34 A. Angerer, S. Enz, M. Ochs and V. Braun, *Mol Microbiol*, 1995, **18**, 163–174.
25
26 35 R. Koebnik, *Trends Microbiol*, 2005, **13**, 343–347.
27
28 36 A. D. Ferguson, C. A. Amezcua, N. M. Halabi, Y. Chelliah, M. K. Rosen, R. Ranganathan
29
30 and J. Deisenhofer, *Proc Nat Acad Sci USA*, 2007, **104**, 513–518.
31
32
33 37 S. Nawapan, N. Charoenlap, A. Charoenwuttitam, P. Saenkham, S. Mongkolsuk and P.
34
35 Vattanaviboon, *J Bacteriol*, 2009, **191**, 5159–5168.
36
37 38 M. Merckx and S. J. Lippard, *J Biol Chem*, 2002, **277**, 5858–5865.
38
39 39 P. A. Phelps, S. K. Agarwal, G. E. Speitel and G. Georgiou, *Appl Environ Microbiol*, 1992,
40
41 **58**, 3701–3708.
42
43 40 M. W. Fitch, D. W. Graham, R. G. Arnold, S. K. Agarwal, P. A. Phelps, G. E. Speitel and
44
45 G. Georgiou, *Appl Environ Microbiol*, 1993, **59**, 2771–2776.
46
47 41 L. Y. Stein, S. Yoon, J. D. Semrau, A. A. DiSpirito, A. Crombie, J. C. Murrell, S.
48
49 Vuilleumier, M. G. Kalyuzhnaya, H. J. M. Op den Camp, F. Bringel, D. Bruce, J.-F. Cheng,
50
51 A. Copeland, L. Goodwin, S. Han, L. Hauser, M. S. M. Jetten, A. Lajus, M. L. Land, A.
52
53
54
55
56
57
58
59
60

- 1
2
3
4 Lapidus, S. Lucas, C. Médigue, S. Pitluck, T. Woyke, A. Zeytun and M. G. Klotz, *J*
5
6 *Bacteriol*, 2010, **192**, 6497–6498.
7
8 42 S. Chillappagari, M. Miethke, H. Trip, O. P. Kuipers and M. A. Marahiel, *J Bacteriol*, 2009,
9
10 **191**, 2362–2370.
11
12 43 F. Serventi, Z. A. Youard, V. Murset, S. Huwiler, D. Bühler, M. Richter, R. Luchsinger, H.-
13
14 M. Fischer, R. Brogioli, M. Niederer and H. Hennecke, *J Biol Chem*, 2012, **287**, 38812–
15
16 38823.
17
18 44 J. S. Cha and D. A. Cooksey, *Appl Environ Microbiol*, 1993, **59**, 1671–1674.
19
20 45 X.-X. Zhang and P. B. Rainey, *Environ Microbiol*, 2008, **10**, 3284–3294.
21
22 46 K. D. Tsirigos, C. Peters, N. Shu, L. Käll and A. Elofsson, *Nucleic Acids Res*, 2015, **43**,
23
24 W401–7.
25
26 47 A. F. El Sheikh, A. T. Poret-Peterson and M. G. Klotz, *Appl Environ Microbiol*, 2007, **74**,
27
28 312–318.
29
30 48 S. Park and R. L. Ely, *Arch Microbiol*, 2007, **189**, 541–548.
31
32 49 F. Arnesano, L. Banci, I. Bertini, S. Mangani and A. R. Thompsett, *Proc Nat Acad Sci USA*,
33
34 2003, **100**, 3814–3819.
35
36 50 S. M. Lee, G. Grass, C. Rensing, S. R. Barrett, C. J. D. Yates, J. V. Stoyanov and N. L.
37
38 Brown, *Biochem Biophys Res Co*, 2002, **295**, 616–620.
39
40 51 L. Zhang, M. Koay, M. J. Maher, Z. Xiao and A. G. Wedd, *J Am Chem Soc*, 2006, **128**,
41
42 5834–5850.
43
44 52 L. A. Abriata, L. Banci, I. Bertini, S. Ciofi-Baffoni, P. Gkazonis, G. A. Spyroulias, A. J.
45
46 Vila and S. Wang, *Nature Chem Biol*, 2008, **4**, 599–601.
47
48 53 K. L. I. M. Blundell, M. A. Hough, E. Vijgenboom and J. A. R. Worrall, *Biochem J*, 2014,
49
50
51
52
53
54
55
56
57
58
59
60

- 1
2
3 459, 525–538.
4
5
6 54 B. P. Dash, M. Alles, F. A. Bundschuh and O. Richter, *Biochim Biophys Acta*, 2015.
7
8 55 C. J. K. Wijekoon, T. R. Young, A. G. Wedd and Z. Xiao, *Inorg Chem*, 2015, **54**, 2950–
9 2959.
10
11
12 56 J. Bengtsson, C. von Wachenfeldt, L. Winstedt, P. Nygaard and L. Hederstedt,
13 *Microbiology*, 2004, **150**, 415–425.
14
15
16 57 P. Greiner, A. Hannappel, C. Werner and B. Ludwig, *Biochim Biophys Acta*, 2008, **1777**,
17 904–911.
18
19
20
21
22 58 Z. Ma, F. E. Jacobsen and D. P. Giedroc, *Chem Rev*, 2009, **109**, 4644–4681.
23
24
25 59 C. Rensing and G. Grass, *FEMS Microbiol Rev*, 2006, **27**, 197–213.
26
27
28 60 C. Rademacher and B. Masepohl, *Microbiology*, 2012, **158**, 2451–2464.
29
30
31 61 S. Ekici, H. Yang, H.-G. Koch and F. Daldal, *mBio*, 2011, **3**, e00293–11–e00293–11.
32
33
34 62 S. Ekici, G. Pawlik, E. Lohmeyer, H.-G. Koch and F. Daldal, *BBA - Bioenergetics*, 2012,
35 **1817**, 898–910.
36
37
38 63 S. Ekici, S. Turkarlan, G. Pawlik, A. Dancis, N. S. Baliga, H.-G. Koch and F. Daldal,
39 *mBio*, 2013, **5**, e01055–13–e01055–13.
40
41
42 64 J. Vandesompele, K. De Preter, F. Pattyn, B. Poppe, N. Van Roy, A. de Paepe and F.
43 Speleman, *Genome Biol*, 2002, **3**, research0034.1.
44
45
46 65 J. Hellemans, G. Mortier, A. de Paepe, F. Speleman and J. Vandesompele, *Genome Biol*,
47 2007, **8**, R19.
48
49
50
51 66 M. B. Eisen, P. T. Spellman, P. O. Brown and D. Botstein, *Proc Nat Acad Sci USA*, 1998,
52 **95**, 14863–14868.
53
54
55 67 A. J. Saldanha, *Bioinformatics*, 2004, **20**, 3246–3248.
56
57
58
59
60

- 1
2
3
4
5
6
7
8
9
10
11
12
13
14
15
16
17
18
19
20
21
22
23
24
25
26
27
28
29
30
31
32
33
34
35
36
37
38
39
40
41
42
43
44
45
46
47
48
49
50
51
52
53
54
55
56
57
58
59
60
- 68 J. P. Bowman and G. S. Sayler, *Biodegradation*, 1994, **5**, 1–11.
- 69 H. Thorvaldsdottir, J. T. Robinson and J. P. Mesirov, *Brief Bioinform*, 2013, **14**, 178–192.
- 70 K. Katoh and D. M. Standley, *Mol Biol Evol*, 2013, **30**, 772–780.
- 71 A. Krogh, B. Larsson, G. von Heijne and E. L. Sonnhammer, *J Mol Bio*, 2001, **305**, 567–580.
- 72 J. Soding, A. Biegert and A. N. Lupas, *Nucleic Acids Res*, 2005, **33**, W244–W248.

Figure legends

Figure 1. The MMO and Mbn operons. (A) The pMMO operon. The order of genes in proteobacterial particulate methane monooxygenase and ammonia monooxygenase is *pmoCAB*; other gene orders occur in some related monooxygenase systems. (B) The sMMO operon. The core sMMO operon (*mmoXYBZDC*) is found adjacent to *mmoR* and *mmoG*, but the order of these genes may vary, and additional operon members are present in some species. (C) The Mbn operon, including a core comprising biosynthesis and export genes (*mbnABCMN*), a group of import genes (*mbn(E)IRT*), and two genes of unknown function (*mbnPH*). (D) Overlap between

1
2
3 sMMO, pMMO/AMO, and Mbn operons in organisms present in the JGI/IMG database. All
4
5 three operons occur independently; no one operon appears to be necessary for either of the others
6
7
8 to function.
9

10
11
12 **Figure 2.** Heatmap of \log_{10} -transformed calibrated normalized relative quantities (CNRQs) for
13 genes obtained via qRT-PCR; downregulation is indicated in blue and upregulation in red.
14
15 Genes were clustered via hierarchical clustering, using Kendall's tau correlation as a similarity
16
17 metric and complete linkage. Genes from each monitored operon cluster with other members of
18
19 the operon, with the exception of regulatory genes from the sMMO and Mbn operons, which
20
21 cluster together as a separate group. Experiments were performed with three biological
22
23 replicates at four timepoints (0 min at $0\mu\text{M}$ CuSO_4 , 15 min at $12.5\mu\text{M}$ CuSO_4 , 5 h at $12.5\mu\text{M}$
24
25 CuSO_4 , and 24 h at $12.5\mu\text{M}$ CuSO_4) for both wildtype *Ms. trichosporium* OB3b and *Ms.*
26
27 *trichosporium* OB3b PP358.
28
29
30
31
32
33
34
35

36
37 **Figure 3.** Phenotypic analysis of qRT-PCR samples. (A) Wildtype (WT) *Ms. trichosporium*
38
39 OB3b spent medium UV-visible spectra. Apo Mbn is visible at 0 min (as shown by the peaks at
40
41 340 and 390 nm); addition of $12.5\mu\text{M}$ CuSO_4 to the medium results in chelation and a shift to a
42
43 typical CuMbn spectrum. (B) Wildtype *Ms. trichosporium* OB3b naphthalene assay for sMMO
44
45 activity. Oxidation of naphthalene by sMMO results in a pink/purple color in the presence of
46
47 Fast Blue B; without sMMO activity, addition of Fast Blue B results in a primarily yellowish
48
49 color. The relevant tubes for the 0 and 15 min timepoints are indicated by black boxes. (C)
50
51 Transmission electron micrographs of wildtype *Ms. trichosporium* OB3b cells. By 5 h and 24 h,
52
53 intracytoplasmic membranes are visible (indicated by arrows). (D) PP358 spent medium UV-
54
55
56
57
58
59
60

1
2
3 visible spectra. Mbn is visible at 0m and is more abundant than in wildtype *Ms. trichosporium*
4
5 OB3b; addition of CuSO₄ to the medium results in chelation and a shift to a typical CuMbn
6
7 spectrum, but by 24 h features at 340 nm and 390 nm are reappearing, indicating that production
8
9 of apo Mbn continues. (E) PP358 naphthalene assay for sMMO activity. Active sMMO remains
10
11 present at all timepoints despite the addition of copper. (F) Transmission electron micrographs of
12
13 PP358 cells. Significant numbers of intracytoplasmic membranes are not observed even at 5 h
14
15 and 24 h.
16
17
18
19

20
21
22 **Figure 4.** Mutation of CopD in the constitutive sMMO-producing PP358 strain. (A) The *copD*
23
24 gene has undergone a multiple-nucleotide frameshift/deletion event. (B) Predicted architectures
25
26 of wildtype and mutated CopD. The last transmembrane helix and the final soluble C-terminal
27
28 domain are predicted to be absent as a result of the deletion.
29
30
31

32
33
34 **Figure 5.** Proposed model for copper homeostasis in *Ms. trichosporium* OB3b.
35
36
37
38
39
40
41
42
43
44
45
46
47
48
49
50
51
52
53
54
55
56
57
58
59
60

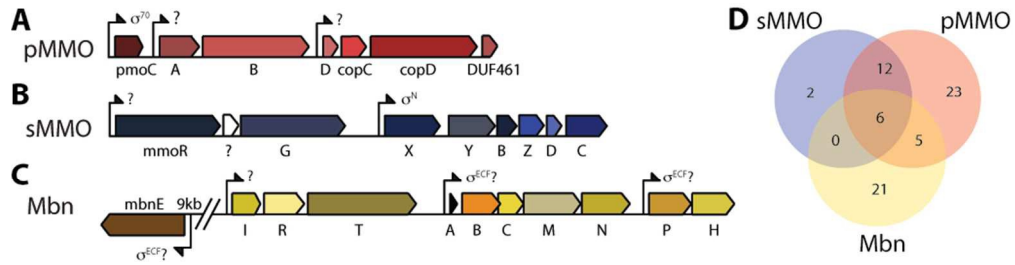


Figure 1
87x22mm (300 x 300 DPI)

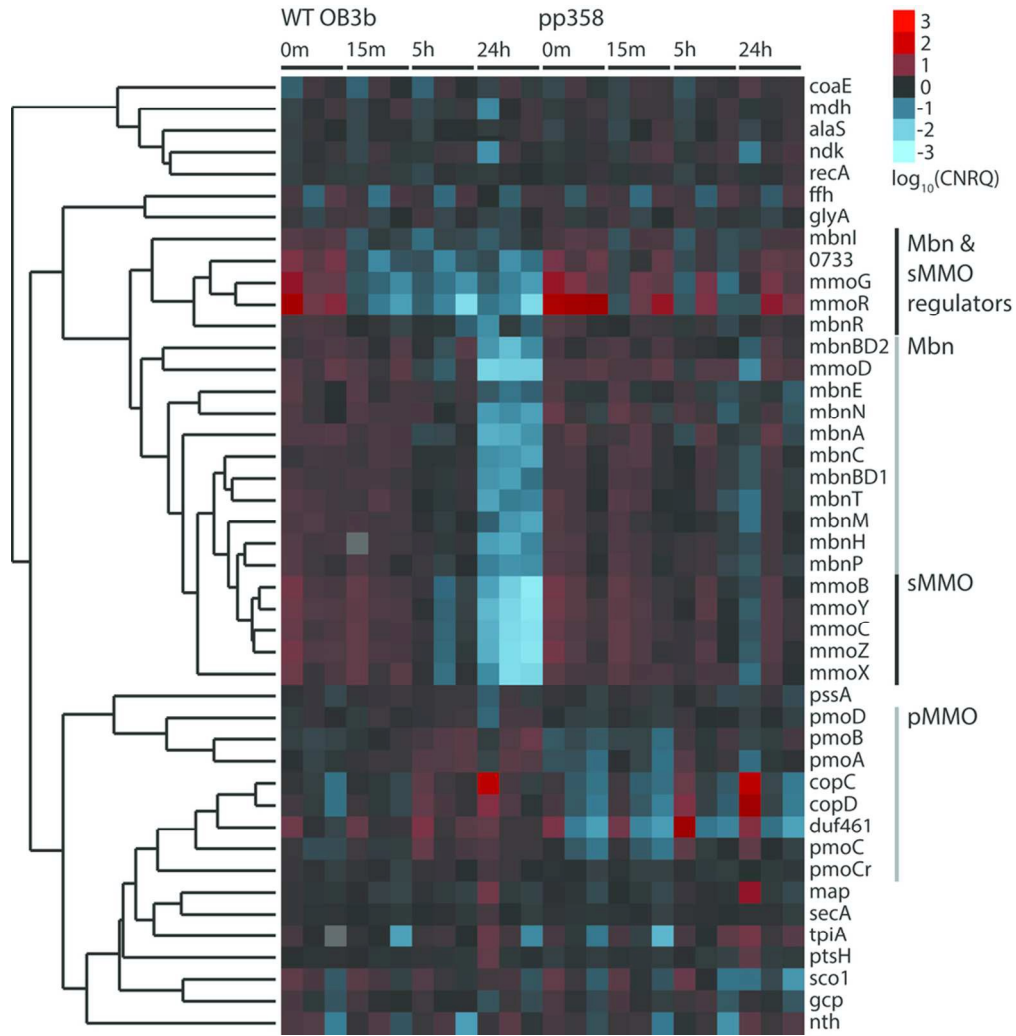


Figure 2
89x91mm (300 x 300 DPI)

1
2
3
4
5
6
7
8
9
10
11
12
13
14
15
16
17
18
19
20
21
22
23
24
25
26
27
28
29
30
31
32
33
34
35
36
37
38
39
40
41
42
43
44
45
46
47
48
49
50
51
52
53
54
55
56
57
58
59
60

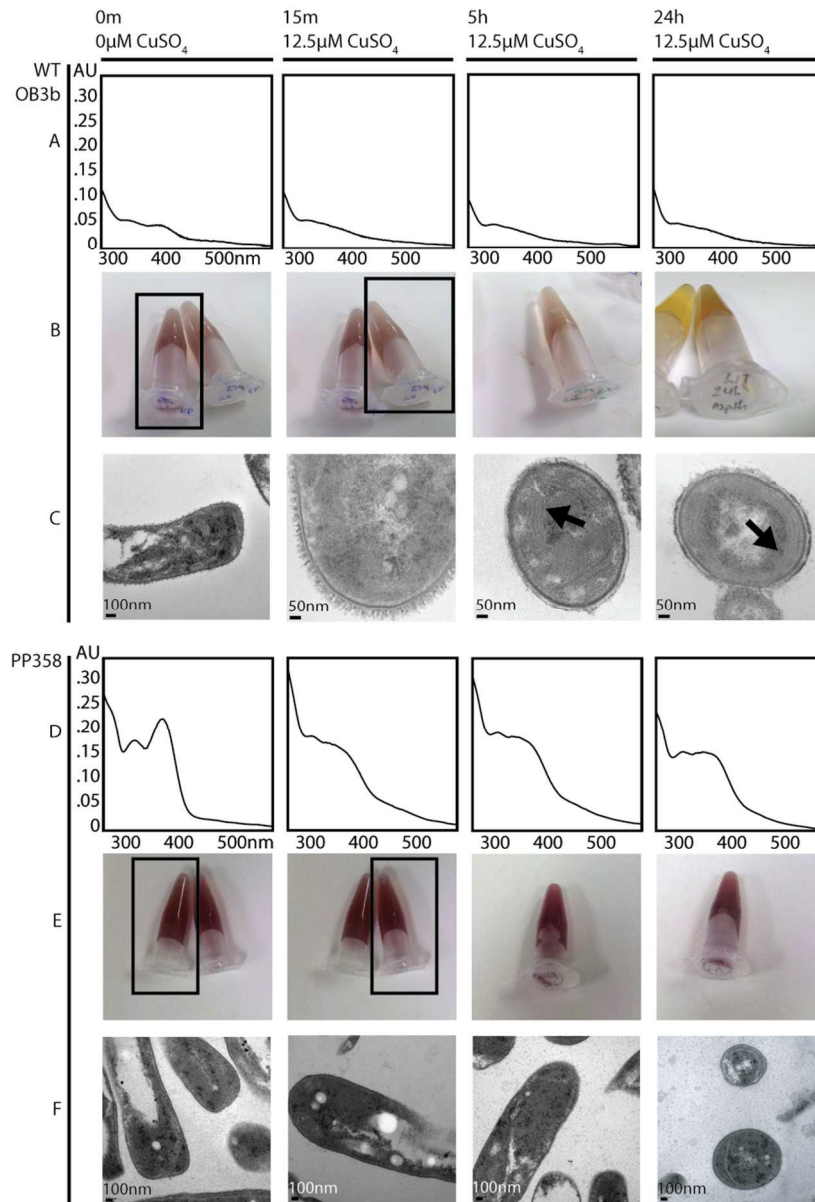


Figure 3
82x120mm (300 x 300 DPI)

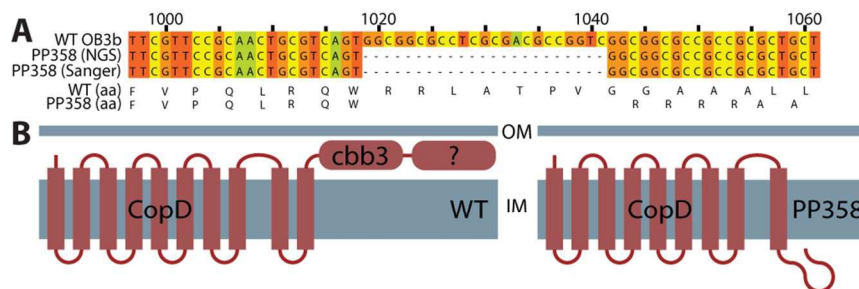


Figure 4
101x51mm (300 x 300 DPI)

1
2
3
4
5
6
7
8
9
10
11
12
13
14
15
16
17
18
19
20
21
22
23
24
25
26
27
28
29
30
31
32
33
34
35
36
37
38
39
40
41
42
43
44
45
46
47
48
49
50
51
52
53
54
55
56
57
58
59
60

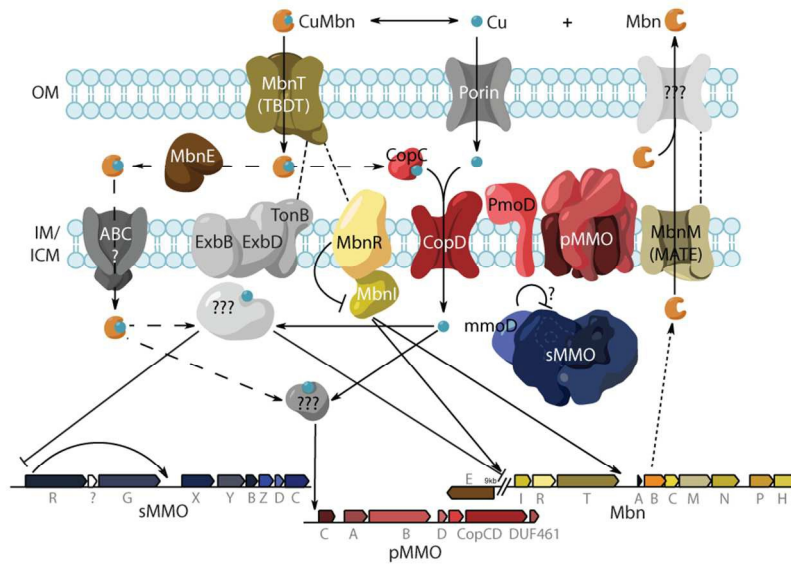


Figure 5
104x83mm (300 x 300 DPI)